Journal of Microscopy, Vol. 221, Pt 2 February 2006, pp. 84–88
Received 11 July 2005; accepted 4 October 2005

Scanning electron microscope imaging in liquids – some data on electron interactions in water

D. C. JOY*† & C. S. JOY*
**Department of Materials Science and Engineering, University of Tennessee, Knoxville, TN 37996, U.S.A.*
†Oak Ridge National Laboratory, Oak Ridge TN 37831, U.S.A.

Key words. Backscattering coefficient, electron range, mean ionization potential, secondary electron yield.

Summary

The electron backscattering coefficient of liquid water has been determined for electrons in the energy range 15–30 keV using Quantomix™ capsules. Values of the mean atomic number for water estimated from a fit to the backscatter yield, the mean ionization potential of water and from Monte Carlo simulations, show that the scattering behaviour of water is not anomalous despite the effects of hydrogen bonding. Computations of the electron range, and of the mean depth for backscattering, in water as a function of incident beam energy show that water and vitreous ice are good media for imaging purposes.

Introduction

There has, understandably, been only a limited amount of experimental work on electron interactions with water (e.g. Schenk *et al.*, 1998) because of the practical difficulty of performing such work in a conventional scanning electron microscope (SEM). However, with the development of the Quantomix™ sealed capsule technology (Thiberge *et al.*, 2004) it is now a matter of routine to use the SEM to image liquids and to image objects immersed in liquids. To properly interpret and optimize such images, however, it is necessary to have quantitative data about the nature of the electron beam interactions involved. The purpose of this note therefore is to report experimental values for the backscattering coefficient for water, and to summarize other relevant data in the literature which can be employed for the simulation of images from an aqueous medium.

Water was chosen for this initial study because of its ubiquity in nature and its convenience as a supporting medium for cells, nanotubes and other small objects. In addition water is an interesting and unusual material because of the effects of hydrogen bonding which result in water being a liquid at room temperatures because its density is much higher than would be predicted from its molecular weight (see e.g. http://www.chemguide.co.uk/atoms/bonding/hbond.html). Although the density of a bulk material does not affect its backscattering coefficient η it is of interest to determine η for liquid water to investigate how this parameter compares with the backscatter yield for some of the other low atomic number materials, such as carbon, that might be encountered in an aqueous environment.

Correspondence to: David C Joy. Tel: 865 974 3642; fax: 865 974 9449; e-mail:djoy@utk.edu

Experimental methods

The measurements reported here were performed in Quantomix™ QX-102 capsules (Quantomix Ltd, Nes-Ziona, Israel). These devices consist of a chamber with a volume of 15 μl sealed from beneath by a polymer O-ring and cap, and sealed on top by a thin membrane stretched across a grid similar to the kind used for transmission electron microscopy. The incident electrons enter, and backscattered electrons leave, the liquid region through the membrane. Measurements were made in a Hitachi S4300 SE-N (Hitachi High Technology, Pleasanton, CA), a variable pressure scanning electron microscope equipped with a Schottky emitter. The instrument was operated with a vacuum of below 10^{-4} Pa in the sample region, as measured by a residual gas analyser. Because the Quantomix™ capsules are completely sealed, low vacuum operation was not found to be necessary for this work. The signal was collected using the large diameter scintillator-type backscatter detector supplied with the instrument and positioned just beneath the objective lens of the microscope.

The principle of the measurement was to measure the backscattering coefficient η by analysing the digital image recorded from the SEM. The signal from the area of interest was compared with the signal from the metal grid supporting the membrane, and with the zero signal level value obtained from temporarily blanking the electron beam by displacing

the aperture. The quantitative analysis was performed using the histogram analysis routines of ImageJ (available as public domain software from http://rsb.info.nih.gov/ij/).

Results

Initial measurements were made on the membranes of empty cells, taking care to ensure that the backscattered electron signal did not clip either the minimum or maximum levels of the recording system. Figure 1 shows a typical image used for this analysis. Histograms were made from multiple regions of interest on the image, each chosen to include portions of the metal grid, the membrane, and the beam blanked regions. This procedure integrates a large number of pixels and so provides excellent statistics. The signal from the beam blanked region records the true zero level of the signal whereas the signal from the grid is proportional to its backscattering coefficient. A quantitative energy dispersive X-ray analysis of the grid material showed it to contain about 17% chrome, 20% nickel and 63% iron. The backscattering coefficient for this composition was then computed as a function of beam energy using Castaing's rule (Castaing, 1960; Heinrich, 1981) with the backscatter coefficients for the individual elements being obtained from the database available online at http://pciserver.bio.utk.edu/metrology. Although this procedure is not ideal, the fact that the major constituents are all of similar atomic number implies that any uncertainties in the estimated backscattered electron (BSE) yield coefficient resulting from errors in the analysed composition will be small. The calculation gave a backscatter coefficient for the grid material of 0.278 at 30 keV, 0.285 at 20 keV and 0.288 at 15 keV.

The backscatter coefficient of the membrane can then be found to a first approximation (Howell *et al.*, 1998) as:

$$\eta_{membrane} = \frac{S_{membrane} - S_{zero}}{S_{grid} - S_{zero}} \cdot \eta_{grid} \qquad (1)$$

where $S_{membrane}$ is the measured signal level from membrane, S_{grid} is the signal from the grid, S_{zero} is the voltage level established by blanking the beam, and η_{grid} is the BSE coefficient for the grid as determined above. The dotted line on Fig. 2 shows the backscatter yields for the membrane as a function of beam energy which were measured in this way.

The information supplied by the manufacturer states that the membrane is a polyimide film about 150 nm in thickness. Assuming that the membrane is actually a variant of Kapton™ (Dupont, Wilmington, DE) for which full chemical and other data can be found at http://www.dupont.com/kapton/general/H-38492-2.pdf then the density is 1.42 g cc^{-1}, and the mean atomic number of the membrane is given as 7.6 by the manufacturer of the cell. Using these estimates the anticipated backscattering coefficient of Kapton™, as a function of beam energy and thickness, was computed using the WinCasino Monte Carlo simulation (Hovington *et al.*, 1997). Bulk Kapton™ at 30 keV is predicted to have a BSE yield of 0.056, and a 150 nm film a BSE yield of 0.0008. The large discrepancy between the measured and the predicted values indicates that the assumption that the measured signal comes only from the membrane is probably incorrect. To investigate this further, several grid squares of membrane were carefully punctured so that the beam could pass directly through them and the experiment was repeated comparing the signal from regions with and without covering. In the absence of the

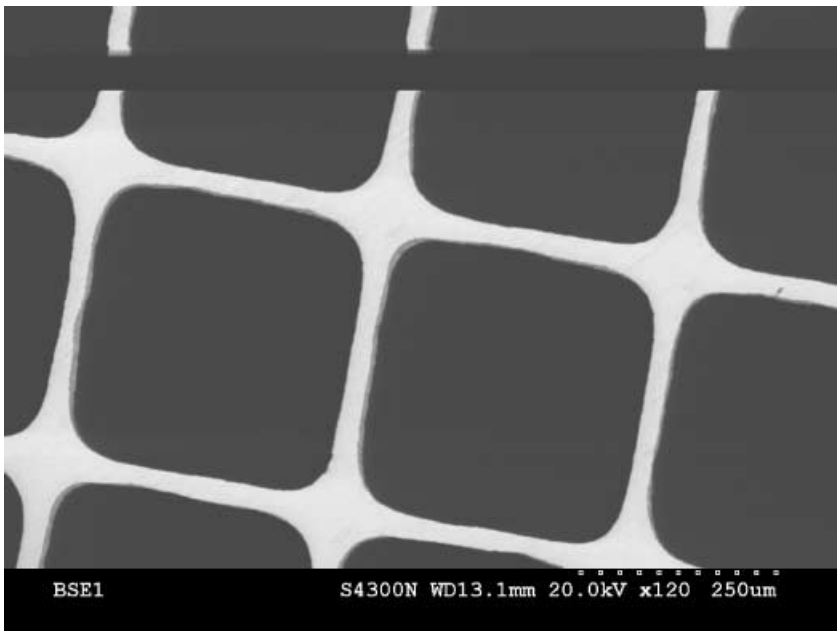

Fig. 1. Backscatter electron image of an empty Quantomix™ capsule recorded at 20 keV. The black band is the result of blanking the incident beam and measures the zero offset in the signal.

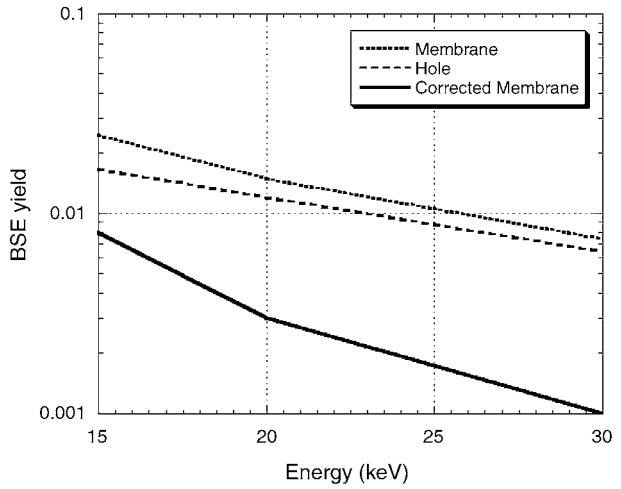

Fig. 2. Measured values of the signal backscattered from the membrane over an empty capsule (dotted line), the scattered signal measured through holes in the membrane (dashed line), and the backscattering coefficient of the membrane after allowing for the scatter component (solid line).

membrane film any backscattered signal is produced by scattering within the empty capsule. As shown by the dashed line in Fig. 2 the signal observed in this condition is a large fraction (70–80%) of the signal previously measured from the membrane, indicating that most of the signal previously measured is the result of the scattering and subsequent re-emergence of electrons transmitted through the membrane. After allowing for this contribution (solid line in Fig. 2) the estimated BSE yield is consistent with that predicted by WinCasino for a Kapton™ film of thickness 150–200 nm. It should be noted that this spurious scattering is, of course, absent when the capsule contains liquid as recommended by the manufacturer.

The Quantomix™ capsules were then filled with distilled, de-ionized water and the measurements repeated. The same procedure as before was employed, calculating the backscatter yield from Eq. (1), but the regions of interest chosen for the histogram measurements must now be chosen with more care. A line trace across a grid bar and into a grid square shows that the backscatter signal dips as the beam approaches the grid bar because a significant fraction of the electrons backscattered by the water are prevented from reaching the surface because of the presence of the grid bar. At 30 keV this region extends more than 20 μm from the edge indicating the order of magnitude of the beam range in water at this energy. Table 1 (second column) shows the measured BSE data from the water-filled cell as a function of energy. The error in the data, representing the spread in values measured from 20 different grid squares selected from three different capsules, is better than 10% relative to the mean value.

This measured backscatter yield is a first approximation to the desired value, but two corrections to the raw result must

Table 1. Experimental data for water.

Energy (keV)	$\eta_{measured}$	$(DQE_{grid}/DQE_{carbon})$	Corrected η_{water}
15	0.050	0.86	0.043
20	0.049	0.83	0.042
30	0.046	0.80	0.038

DQE, detector quantum efficiency.

be considered in order to determine a final value. First, the value measured includes a contribution from the membrane over the liquid. However, as seen from Fig. 2, at 30 keV the additional signal from the Kapton™ membrane is insignificant, whereas at 15 keV the contribution is still only about 10%. In practice even this estimate is too high because, for a given beam energy, placing a thin layer of some material A on top of a bulk sample of material B will result in a change of backscattering that depends on the difference in yield from the layer A and the yield from an equivalent thickness of the substrate B. As water and the Kapton™ both have relatively low atomic numbers this differential effect will be very small. Consequently in the energy range 15–30 keV the contribution from the membrane to the final result is taken to be negligible.

A second issue is the validity of Eq. (1) which assumes that the detected backscatter signal is proportional only to the backscatter yield. Although this approximation has been commonly used (Howell *et al.*, 1998), for studies on materials of widely different atomic number and for most backscatter detectors, this assertion may not be true because the signal out of the detector will depend not only on the number of BSEs collected (i.e. the yield) but also on the energy of these BSEs. The energy distribution of BSE from low atomic number and high atomic number materials is different (Thiberge *et al.*, 2004; Goldstein *et al.*, 2005) so the same number of BSE striking the detector but coming from materials of different atomic number Z – such as from water and from a metal grid – would in general result in different output signals. This effect can be accounted for by experimentally measuring the BSE detector quantum efficiency (DQE) for the materials and energies of interest (Joy *et al.* 1996a). Equation (1) then takes on a modified form:

$$\eta_{unknown} = \frac{S_{unknown}}{S_{standard}} \cdot \left(\frac{DQE_{standard}}{DQE_{unknown}} \right) \cdot \eta_{standard} \qquad (2)$$

where $\eta_{unknown}$ and $\eta_{standard}$ are, respectively, the backscattering coefficients of the material being measured and some known material standard, $S_{unknown}$ and $S_{standard}$ are the corresponding signals measured from the backscattered detector, and $DQE_{standard}$ and $DQE_{unknown}$ are the detector quantum efficiency of the BSE detector at the beam energy of the experiment for the two materials examined. Equation (2) cannot be used directly in the form given because a measurement of the detector DQE

(Joy *et al.* 1996a) for the unknown itself requires a knowledge of $\eta_{unknown}$. In this case therefore the DQE of the BSE detector was measured at 15, 20, and 30 keV for pure carbon – assumed for the purposes of this experiment to be approximately equivalent to water – and for the grid material. The measured ratio of DQE_{grid}/DQE_{carbon} is tabulated in the third column of Table 1 and is seen to differ from unity. As a result the signal from the grid material is being weighted less strongly than it should be and so the correction of Eq. (2) must be applied. The fourth column of Table 1 then gives the final estimate of the backscattering coefficient after allowing for the material-dependent DQE variation. The precision of the measurement, based on the replicates performed, was better than 10%. These values are comparable with, but rather lower than, those of Thiberge *et al.* (2004) obtained with a somewhat different measurement technique. For comparison, at 30 keV the BSE yield of Be ($Z = 4$) is 0.039, for B ($Z = 5$) is 0.043 and for C ($Z = 6$) is 0.055 (data from references in http://pciserver.bio.utk.edu/metrology) so good imaging contrast between most low Z materials and water will be obtained.

For comparison this same sequence of measurements was repeated using saline solution (Bausch and Lomb, Rochester, NY) instead of pure distilled water. An analysis of the results gives the backscattering coefficient of saline as 0.047 (at 15 keV), 0.045 (at 20 keV) and 0.042 (at 30 keV). The backscatter yield is thus approximately 10% higher than that of water alone, a value which seems consistent with the slightly higher atomic number of the solution.

A summary of other data on electron interactions in water

When using the Quantomix™ capsule there is no possibility of measuring a secondary electron signal from the water through the membrane, but it is of interest to note that the secondary electron yield of liquid water as a function of beam energy has been measured by Thiel *et al.* (1999), and also by Hilleret *et al.* (2000) who examined 200 monolayers of water on a copper substrate. The secondary electron yield of ice has been measured by Suszcynsky *et al.* (1992). For convenience these results are summarized in Fig. 3 which shows that there is good general agreement between the values obtained and that, as would be anticipated, the properties of vitreous ice are closely similar to those of water.

Although physically the concept is not easy to justify the 'effective mean atomic number' Z_{av} is a quantity commonly used to approximate the behaviour of a compound in applications such as Monte Carlo modelling (Joy, 1996; Howell *et al.*, 1998) and electron beam microanalysis (Goldstein *et al.*, 2005). Based on the data assembled here several estimates of Z_{av} for water can be made. Hunger & Kuchler (1979) have given an empirical relationship between the backscattering coefficient η, the incident beam energy E, and the atomic number Z which is a good fit for a wide range of Z and E-values and has the form

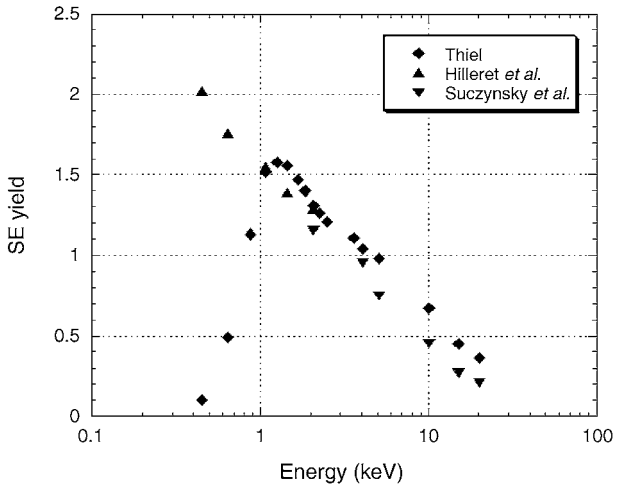

Fig. 3. The secondary electron yield from water (Thiel *et al.*, 1999; Hilleret *et al.*, 2000) and from vitreous ice (Suszcynsky *et al.*, 1992) as a function of incident beam energy.

$$\eta(Z,E) = E^{m(Z)} \cdot C(Z) \qquad (3)$$

where $m(Z) = 0.1382 - (0.9233/Z^{0.5})$ and $C(Z) = 0.1904 - 0.2236\ln(Z) + 0.1292(\ln(Z))^2 - 0.01491(\ln(Z))^3$

A spreadsheet numerical solution for Z applying Eq. (3) to the BSE yield data in Table 1 gives a value for Z_{av} as 4.6 for the range 15–30 keV.

The stopping power of electrons in vitreous ice has been calculated by Ashley (1982) and also by Mozumder & LaVerne (1985), and measured by Luo *et al.* (1991). A Fano plot analysis of the experimental data (Joy *et al.*, 1996b) shows that for electron energies above about 300 eV the mean ionization potential J is 77 eV which compares well with the I.C.R.U. (1983) value, determined by MeV energy β-particle irradiation, of 75 eV and also with the theoretical predictions. The mean ionization potential J as a function of atomic number is represented (Berger & Seltzer, 1964) by the expression

$$J = 9.76Z + \frac{58.5}{Z^{0.19}} \qquad (4)$$

A spreadsheet numerical solution of Eq. (4) for the J-value of 77 eV then gives Z_{av} as 3.1.

Finally, using the measured value of J for the stopping power but treating Z_{av} as a free variable in several Monte Carlo simulations (Joy, 1996; WinCasino from Hovington *et al.*, 1997; the Metrologia version (SPECTEL; San Jose, CA) of the NIST 'MONSEL' code (Lowney, 1995)), shows that a value of 4.4 for Z_{av} gives the best fit to the experimental backscattering yields in Table 1. These three estimates are thus in general agreement with the expected value from the chemical formula which gives Z_{av} as 3.3 indicating that, within the admitted limitations of such empirical fits as those applied here, the behaviour of water is as expected.

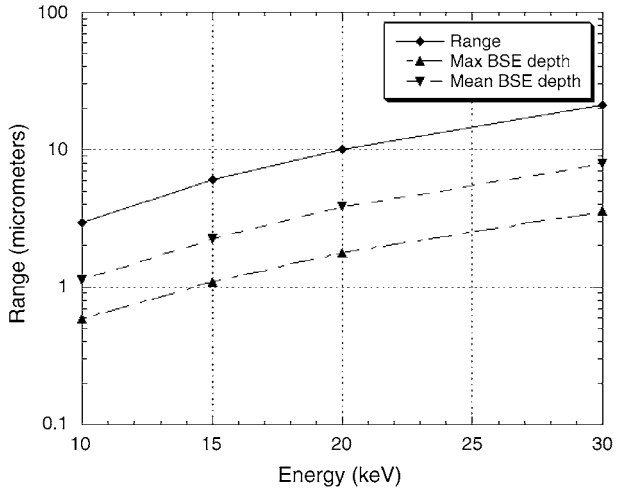

Fig. 4. The range of electrons in water (solid line), the mean depth from which electrons are backscattered (dashed line), and the maximum depth from which electrons are backscattered (dot-dash line) in water as a function of incident beam energy. Data computed from Monte Carlo simulations using the parameters derived and tabulated in the text.

These values can now be used to predict details of electron interactions with water. For example, Fig. 4 plots the electron range in water as a function of energy, together with estimates of the mean depth from which electrons are backscattered and the maximum depth from which any electron is backscattered derived from Monte Carlo models. The low density of water results in both a relatively large range (over 20 μm at 30 keV) and a high mean depth for backscattering. BSE imaging in water at incident energies in the range 15–30 keV will therefore allow the visualization of structures many micrometers beneath the liquid surface. Estimates of the imaging resolution that can be expected as a function of depth and energy indicate that 100 nm or better can be achieved in many situations, depending on the depth and on the inherent contrast of the feature being examined. Because vitreous ice has the same density as liquid water and very similar electron scattering properties, comparable performance would be expected for that matrix.

Conclusions

The electron backscattering coefficient for liquid water has been measured to be in the range 0.038 at 30 keV to 0.043 at 15 keV beam incident energy. Estimates based on the backscattering coefficient, the tabulated stopping power, and on Monte Carlo simulations show that the effective atomic number of water (and ice) is in the range 3.1–4.4. Electron range data and a value for the mean depth from which electrons in water are backscattered have been calculated and confirm that water is an excellent medium for imaging in the SEM. Published images taken in water using the Quantomix™ cell (e.g. Thiberge *et al.*, 2004; see also http://www.quantomix.com/dwnlds/qx_technology.pdf) demonstrate that this is indeed the case.

Acknowledgements

The authors are grateful to Dr Jim FitzGerald (University of Virginia) and Dr Niels de Jonge (Oak Ridge National Laboratory) for helpful discussions. Oak Ridge National Laboratory is managed by UT-Battelle, LLC for the U.S. Department of Energy under contract number DE-AC05–00OR22725.

References

Ashley, J.C. (1982) Stopping power of liquid water for low energy electrons. *Rad. Res.* **89**, 25–32.

Berger, M.J. & Seltzer, S.M. (1964) Studies in penetration of charged particles in matter. *Nucl. Sec. Ser. Rep.* 39, NAS-SRC, Washington DC, 205.

Castaing, R. (1960) Electron probe microanalysis. *Adv. Electron. Electron Phys.* **13**, 317–385.

Goldstein, J., Newbury, D.E., Joy, D.C. *et al.* (2005) *Scanning Electron Microscopy and X-Ray Microanalysis*, 3rd edn. Kluwer Academic/Plenum Publishers, New York.

Heinrich, K.F.J. (1981) *Electron Beam Microanalysis.* Van Nostrand, New York.

Hilleret, N., Bojko, J., Grobner, O., Henrist, B., Scheuerlein, C. & Taborelli, M. (2000). Personal communication of paper *The secondary electron yield of technical materials and its variation with surface treatments.* Presented at 7th European Particle Accelerator Conference, Vienna.

Hovington, P., Drouin, D. & Gauvin, R. (1997) CASINO A New Monte Carlo code in C language. *SCANNING*, **19**, 1–14.

Howell, P.G.T., Davy, K.M.W. & Boyde, A. (1998) Mean atomic number and backscattered electron coefficient for some materials of low mean atomic number. *SCANNING*, **20**, 35–40.

Hunger, H.J. & Kuchler, L. (1979) Measurements of electron backscattering coefficient for quantitative EPMA in the energy range 4–4 0keV. *Phys. Stat. Sol (A)*, **56**, K45–K48.

I.C.R.U. (1983) *Stopping Powers of Electrons and Positrons*. Report 37 to the International Committee on Radiation Units. ICRU, Bethesda, MD.

Joy, D.C. (1996) *Monte Carlo Modeling for Microscopy and Microanalysis.* Oxford University Press, New York.

Joy, D.C., Joy, C.S. & Bunn, R.D. (1996a) Experimental measurements of the efficiency, and static and dynamic response of electron detectors in the SEM. *Scanning*, **18**, 181–190.

Joy, D.C., Luo, S., Gauvin, R., Hovington, P. & Evans, N. (1996b). Experimental measurements of electron stopping power at low energies. *Scan. Microsc.* **10**, 653–666.

Lowney, J. (1995) MONSEL II – Monte Carlo simulation of SEM signals for linewidth metrology. *Microbeam Anal.* **4**, 131–136.

Luo, S., Zhang, X. & Joy, D.C. (1991) Experimental measurements of electron stopping power. *Rad. Eff. Defects Solids*, **117**, 235–247.

Mozumder, A. & LaVerne, J.A. (1985) Range and range straggling of low energy electrons – general considerations and applications for N_2, O_2, and H_2O. *J. Phys. Chem.* **89**, 930–936.

Schenk, M., Futing, M. & Reichelt, R. (1998) Direct visualization of a water mensicus by SEM. *J. Appl. Phys.* **84**, 4880–4884.

Suszcynsky, D.M., Borovsky, J.E. & Goertz, C.K. (1992) Secondary electrons yields of solar system ices. *J. Geophys. Res.* **97** (E2), 2611–2619.

Thiberge, S., Zik, O. & Moses, E. (2004) An Apparatus for imaging liquids, cells, and other wet samples in the SEM. *Rev. Sci. Instrum.* **75**, 2280–2289.

Thiel, B.L., Stokes, D.J. & Phifer, D. (1999) Secondary electron yield of water. *Microsc. Microanal.* **5** (Suppl. 2), 282–283.